M Bosio, Andrea Belleri, P Riva, A Marini. 2020. "Displacement-Based Simplified Seismic Loss Assessment of Italian Precast Buildings". Journal of Earthquake Engineering, Vol.24:sup1, pp.60-81 . DOI: 10.1080/13632469.2020.1724215
Publisher's version at: https://doi.org/10.1080/13632469.2020.1724215

Displacement-Based Simplified Seismic Loss Assessment of Italian Precast Buildings

Marco Bosio[1], Andrea Belleri[2], Paolo Riva[3], Alessandra Marini[4]

[1] PhD student, Department of Engineering and Applied Sciences, University of Bergamo, Bergamo, Italy

[2] Assistant professor (corresponding author: andrea.belleri@unibg.it), Department of Engineering and Applied Sciences, University of Bergamo, Bergamo, Italy

[3] Professor, Department of Engineering and Applied Sciences, University of Bergamo, Bergamo, Italy

[4] Associate professor, Department of Engineering and Applied Sciences, University of Bergamo, Bergamo, Italy

Abstract

Economic losses associated with the structural and non-structural damage occurring after an earthquake are of particular importance in the case of industrial buildings due to the consequences of such losses on the local economy and employment level. The seismic sequences that hit the industrial area of Emilia-Romagna region of Italy in 2012 represent an emblematic example. In this earthquake event, major damage on poorly performing precast structures was recorded: many buildings were severely damaged and experienced partial or full collapse. The level of the recorded damage was related to a design lacking modern seismic detailing and to a non-up-to-date evaluation of the seismic hazard: in fact, several industrial buildings, typically one storey precast reinforced concrete (RC) structures, were designed to transfer horizontal loads (i.e. between roof elements and supporting beam or main girder and supporting columns) through either friction or under-designed mechanical connections.

The aim of this paper is to provide insights on the evaluation of direct losses in the case of precast RC structures typical of the Italian industrial sector, particularly for buildings built before the enforcement of modern seismic codes. A simplified displacement-based seismic loss assessment procedure is proposed and applied to a selected case study and comparisons are made with the results obtained from non-linear time history analyses on simplified (i.e. single column models) and complete three dimensional models. Retrofit solutions are proposed and their influence on the collapse probability of the structural elements and on the economic losses is evaluated.

Keywords:

Displacement based assessment; seismic losses; precast structures; precast connections;

1. Introduction

Recent earthquakes in Italy (L'Aquila 2009, Emilia 2012, Central Italy 2016) have highlighted the vulnerability of precast reinforced concrete (RC) structures not designed according to modern seismic regulations [Toniolo et al 2012; Savoia et al. 2012; Magliulo et al. 2014a; Belleri et al. 2014; Bournas et al. 2014; Minghini et al. 2016; Nastri et al. 2017; Palanci et al. 2017]. The main vulnerabilities, which have caused both local and global collapses, are related to the lack of an effective horizontal transfer mechanism enabling horizontal load transferring between prefabricated elements and to the absence of displacement and rotation compatibility between structural elements and among structural and non-structural elements [Belleri et al. 2014; Belleri et al. 2015; Brunesi et al. 2015; Casotto et al. 2015; Colombo et al. 2016; Demartino et al. 2018]. Industrial and commercial precast buildings are generally characterized by a greater inter-storey height and greater in-plane flexibility of the roof [Belleri et al. 2015; Dal Lago et al. 2019] compared to traditional RC buildings: this leads to a global higher lateral flexibility which makes the compatibility of displacements and rotations between connected elements a fundamental aspect to be assessed.

The considered precast buildings, typical of the Italian existing building stock, are characterized by a simple structural layout with cantilever columns pin-connected to pre-cast pre-stressed beams supporting roof elements. Columns are either placed in pocket footings or connected to the foundation by means of mechanical devices or grouted sleeves [Belleri et al. 2012; Dal Lago et al. 2016]. In the past, the beams were either simply supported on the columns, or connected to them through dowels embedded in the column and grouted in a beam pocket [Magliulo et al. 2014b; Zoubek et al. 2015; Kremmyda et al. 2017; Clementi et al. 2016]. The building closure system is generally made up of precast RC panels. The mechanical system connecting the panels to the load-bearing structure was designed primarily to withstand gravity, wind loads or, more recently, to prevent out-of-plane failure due to seismic loads. The connections were supposed to be able to collect the relative displacements and rotations between the panels and the supporting structure, due to the lower stiffness of the connections with respect to the connected prefabricated elements [Bournas et al. 2014; Scotta et al. 2015; Belleri et al. 2016; Belleri et al. 2017a; Colombo et al. 2016; Zoubek et al. 2016].

During the last two decades, many researchers have focused their research activity on examining the effects of the earthquake in terms of losses (typically causalities, downtime, and economic loss). Among these studies, the performance-based earthquake engineering methodology developed at the Pacific Earthquake Engineering Research centre, known as PEER-PBEE, is the methodology most commonly used for these analyses. The PEER-PBEE procedure allows to estimate the seismic performance of a structural system in terms of direct and indirect losses; it consists of four macro-phases: hazard analysis, structural analysis, damage analysis and finally loss analysis [Günay et al.

2012; Krawinkler et al. 2004; Kunnath et al. 2006]. Through the application of the total probability theorem it is possible to determine the curve of the expected losses for a specific structure as a function of the frequency of occurrence and, through its integral, the value of the expected annual losses.

In the past, various researchers made an attempt to provide simplified version of the PEER-PBEE procedure for professional applications [FEMA P-58-3.1 2012; Papadopoulos et al. 2019; Cremen et al. 2019; Del Vecchio et al. 2018; Xu et al. 2019; Welch et al. 2015; Sullivan 2016; Baltzopoulos et al. 2017]. The present paper considers the displacement-based approach developed by Priestley et al. (2007) and previously applied to the design and assessment of RC precast buildings [Belleri 2017; Torquati et al. 2018] as the basis for the seismic loss assessment of this structural typology. The procedure is applied to simplified models for selected limit states. The results are validated against those obtained from a more refined approach considering non-linear time history analyses and several limit states; both simplified models (i.e. single column models) and complete three-dimensional models are considered. A collapse hierarchy chain is introduced and the influence of various retrofit strategies is also evaluated in terms of variation of the expected annual losses (EAL) and variation of the local collapse probability.

2. DBLA framework and specific considerations for precast buildings

The displacement based loss assessment (DBLA) method [Welch et al. 2014] is based on the direct displacement-based design approach proposed by Priestley et al. (2007). The procedure considers the lateral displacements of the building as the main parameter for the seismic assessment of the structure. The lateral displacements are suitable seismic vulnerability indicators for the considered structural typology, owing to the high deformability of the structural system combined with the high deformation demand in the connection region. In the case of precast structures with non-emulative connections [Torquati et al. 2018] the assessment follows these steps:

1. Choice of the most appropriate inelastic deflected shape
2. Definition of a force-displacement capacity curve
3. Selection of the target displacement at a given limit state (LS)
4. Definition of the equivalent single degree of freedom (SDOF) structure
5. Evaluation of the equivalent viscous damping and displacement spectrum reduction factor
6. Evaluation of the damped displacement spectrum
7. Computation of the annual probability of exceedance associated with the selected limit state

The most appropriate deflected shape is a function of the type of beam-column connections and it can be obtained from a pushover analysis or from the equivalent column simplified method (ECSM)

reported in Torquati et al. (2018). In the present paper, the first method is addressed and the interested reader is referred to the aforementioned research paper for insights on the displacement-based assessment procedure applied to precast RC structures with non-emulative connections. The term "emulative" connections refers to precast connections able to provide the same degree of continuity and strength of cast in place RC structures. "Not-emulative" connections are generally dry-assembled connections with a lower degree of fixity compared to cast in place RC connections, typically pinned connections.

The evaluation of economic losses at selected limit states (typically associated with a probability of exceedance in the reference period equal to 81%, 63%, 10%, and 5%, corresponding to the fully operational, serviceability, life safety and collapse prevention limit states - LS, respectively) is carried out by considering the corresponding engineering demand parameter (EDP) of the structural and non-structural elements and by evaluating the related repair costs for selected damage states, similarly to the loss analysis of the PEER-PBEE procedure. Once the economic losses have been derived, the expected annual loss (EAL) is obtained from the integral of the loss curve connecting the selected limit states [Welch et al. 2014] and described in O'Reilly et al. (2019). To account for uncertainties in the demand and capacity the SAC-FEMA approach of Cornell et al. [2002], simplified according with the recommendations by Fajfar and Dolsek [2010], is considered.

The evaluation of the economic losses due to a seismic event is an important tool for assessing the seismic risk of existing buildings. However, in the case of precast industrial and commercial buildings, the loss estimation procedure is influenced by the presence of local vulnerabilities which may trigger local collapses: indeed, unlike traditional RC buildings, precast buildings cannot be regarded as monolithic structures; in addition, the connection between structural components is guaranteed by mechanical devices or by friction.

As observed in past earthquakes, especially in the Emilia 2012 seismic sequence that hit industrial areas with several RC precast structures, the local vulnerabilities may substantial affect the global structural performance. In fact, the failure of an element can be associated with the failure of the element itself or with the failure of its supporting elements. A typical example is given by the roof elements, where collapse can occur due to an excessive sliding on the support (i.e. loss of support), or due to failure of one of the supporting beams or supporting columns. In traditional RC buildings, the collapse of a structural element does not necessarily lead to the collapse of what it supports, as different load paths are possible due to the inherent structural redundancy typical of monolithic structures. In the considered structural typology, this is rarely possible due to a static scheme resembling a statically determinant structure; therefore, the failure of an element induces the collapse of everything that is supported by the element itself.

When analysing this type of structures, it is therefore essential to determine the collapse hierarchy of the building, which can be represented by a logical tree that identifies those elements whose damage/collapse may influence the collapse of other portions of the structure (**Figure 1**). It is observed that the columns are at the lowest level of the collapse hierarchy with a failure typically associated with the flexural failure of the plastic hinge at their base. Each column influences the damage of the horizontal cladding panels and of the beam-column connection which, in turn, affects the damage to the beam. Each beam influences the damage to the connected vertical panels and to the supported roof elements. From the collapse hierarchy, it is possible to define a procedure able to determine the expected losses due to a seismic event: when the damage is governed by local collapses, it is important to avoid counting repeatedly the losses associated with the same element. This procedure is presented in **Figure 1**.

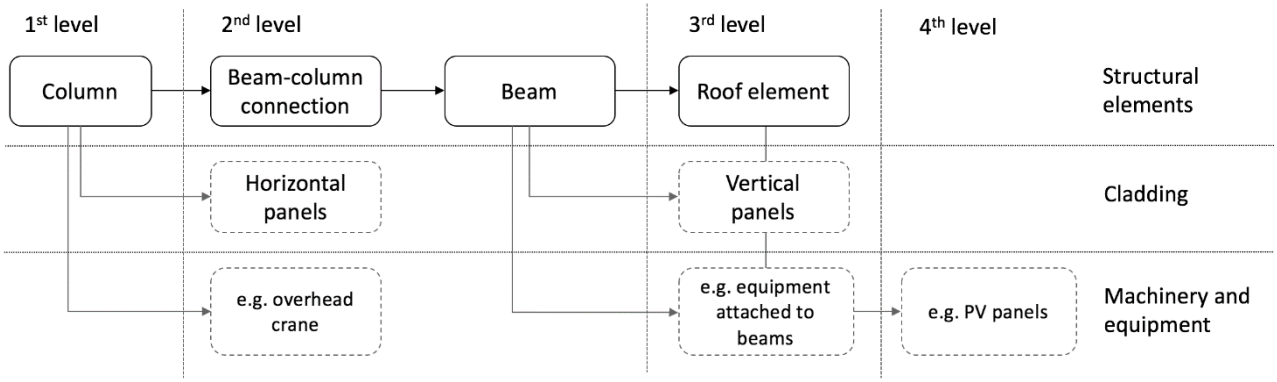

Figure 1 – Example of collapse hierarchy for precast industrial buildings

To this end, it is suggested to subdivide a precast building into every single element or substructures for which a potential vulnerability is detected and the probability of damage is determined. Two different damage probabilities are defined: the first one is calculated on the basis of the engineering demand parameter associated with the damage of the analysed element, the second one takes into account the collapse hierarchy to determine the probability of global damage considering all the elements whose collapse influences the failure of the selected element.

The definition of the damage probability of the element itself, i.e. without considering the influence of the supporting structure, is obtained from considering the fragility curves of the identified vulnerabilities given the most relevant EDP of the element. Typically, a lognormal distribution is considered and the probability of exceeding a given damage state is thus calculated once the mean value of the damage state and its dispersion have been defined. In this way, it is possible to define the probability of selected damage states for all the elements, given the associated EDP; these values are the starting point for determining the "global damage" to the element, which also accounts for the probability of collapse of the underlying elements in the collapse hierarchy.

The procedure starts from the elements located in the highest level of the collapse hierarchy, whose failure does not influence the collapse of other elements. The probability of damage of such elements depends on the selected EDP, given that the failure is avoided in the collapse chain of the supporting elements. For example, to determine the probability of damage of a roof element it will be necessary to compute the probability of the selected damage state as a function of the EDP and the probability of no collapse of the supporting beam, which in turn takes into account the probability of no-collapse of the dowel connection and the probability of no collapse of the columns, until the bottom of the collapse hierarchy is reached. Considering the failure of each supporting element as an independent variable, the probability of exceeding a given damage state for a selected element is therefore:

$$P_{DS-i}^{G} = P_{DS-i}^{L} \cdot \prod P_{NC-sup}^{G} \quad (3)$$

where P_{DS-i}^{G} represents the global probability of exceedance of the ith damage state of the selected element; P_{DS-i}^{L} represents the local probability of exceedance of the ith damage state of the selected element; $\prod P_{NC-sup}^{G}$ represents the product of the probability of no-collapse of the supporting elements in the collapse chain: $P_{NC-sup}^{G} = 1 - P_{C-sup}^{G}$, being P_{C-sup}^{G} the collapse probability.

Through the application of these equations, it is possible to determine the overall probability of exceeding the various damage states identified for each element. The proposed formulation is fundamental in the case of local collapses. At this regard, **Figure 2** shows an example of application to the roof elements: **Figure 2a** shows the single-element collapse probability evaluated considering only the relevant EDP value for each element, while **Figure 2b** shows the collapse probability of the roof elements taking into account the collapse probability of all the supporting elements in the hierarchy chain. It can be observed that, in the first case (i.e. single-element collapse probability; **Figure 2a**), about half of the roof elements have a collapse probability equal to zero, since the relative sliding (i.e. the selected EDP) between them and the supporting beam is negligible, while in the second case (i.e. global collapse probability; **Figure 2b**) all the roof elements collapse due to failure of the supporting elements. Therefore, there would be a significant underestimation of the losses by evaluating the collapse probability on a single-element basis.

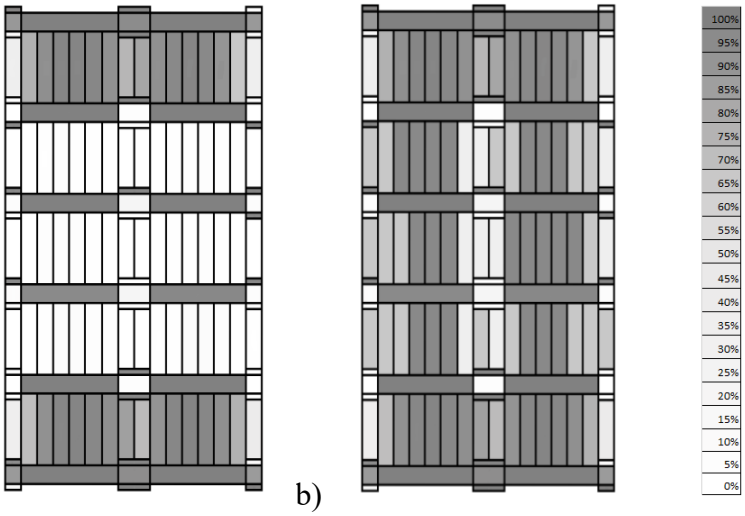

a) b)

Figure 2 – Collapse probability of the roof elements considering the sole element EDP (a) and the collapse hierarchy chain (b)

From the application of the proposed procedure it is possible to evaluate the probability of exceeding selected damage states for all the elements. The economic losses (L_j) of each element are obtained from the following equation:

$$L_j = \left[\sum_{i=1}^{I-1} \left(P^G_{DS-i,j} - P^G_{DS-i+1,j} \right) \cdot C_{DS-i,j} \right] + P^G_{DS-I,j} \cdot C_{DS-I,j} \quad (4)$$

where i represents the i^{th} damage state, I is the last damage state (herein taken as the failure of the element), j represents the considered j^{th} element, $P^G_{DS-i,j}$ is the global probability of exceedance for the i^{th} damage state of the j^{th} element, and $C_{DS-i,j}$ is the repair cost for the i^{th} damage state of the j^{th} element. It is worth noting that in the case of collapse of a given element, the portion of **Eq. 4** contained in the squared brackets is zero. The total losses are obtained from summing the losses of each element. In the following case study an average repair cost is defined for each damage state and is applied without considering dispersions due to possible variations of market prices and labour cost.

3. Case study

The building chosen as a case study well-represents the typical small-medium size precast industrial building in the Italian territory with structural details not accounting for anti-seismic regulations. The single-storey building has a plan dimension of 15m x 24m and it is characterized by a single span along the short direction and four bays along the orthogonal direction. The 6m height columns have a 0.5m x 0.5m square cross-section; the longitudinal reinforcement is arranged by grouping two 20mm diameter bars at each corner and 6mm diameter stirrups with 200mm spacing. A column corbel is placed at 4.5m height to support the runway beams (type HEB 400) of the overhead crane. The

latter has a mass of 5000kg and a payload of 9kN. The foundation is made of spread cup footings. The considered average strength of the concrete is 53MPa and the yielding strength of the steel is 550MPa.

The main beams are made of RC pre-stressed elements with variable cross-section (**Figure 4**). The beam-column connection is made of two 14mm diameter dowels (with yielding strength equal to 300MPa) protruding from the columns, inserted into vertical tubes at the beam-ends and subsequently filled with grout. A 20mm neoprene pad is placed on the beam-column contact surface to distribute the gravity loads. The roof is made of double-tee RC pre-stressed elements (**Figure 4**) with no mechanical connections to the supporting beams. Regarding the lateral closures, the building has vertical cladding panels simply-supported on the ground floor and connected to the main beams along the building transversal direction, while 3 horizontal cladding panels connect each set of adjacent columns along the building longitudinal direction.

The building is considered located at L'Aquila on soil type A [D.M. 14/01/2008For the non-linear time history analyses, 9 sets of 10 accelerograms with increasing intensity were selected according to the conditional mean spectrum procedure [Baker 2011] for the period 1.5s, as described in O'Reilly et al. (2019). More details on the input ground motions are in the Appendix.

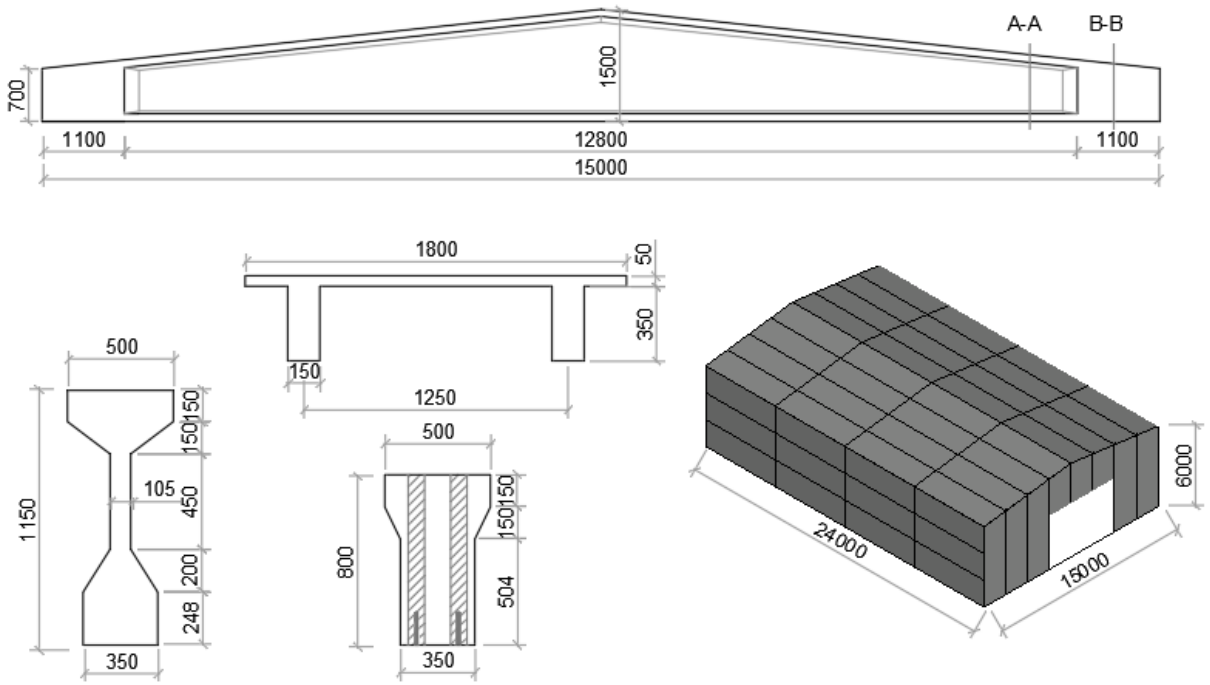

Figure 3 – Case study main geometry characteristics. Note: dimensions in mm.

The finite element modelling (**Figure 6**) was performed in OpenSees [McKenna and Fenves 2013] considering the non-linear behaviour of the main elements. The plastic hinge at the column base and the beam-column dowel connection were modelled by means zero-length elements with hysteretic behaviour according to the modified Ibarra-Medina-Krawinkler deterioration model with bilinear

hysteretic response and no cycle degradation [McKenna et al. 2013]. The main parameters of the model are reported in **Table 1** and they have been derived in accordance to what reported in Magliulo et al. [2018]. Regarding the beam-column dowel connections, the dowel failure was assumed equal to twice the bar diameter as inferred from experimental tests [Kremmyda et al. 2014]. In addition, a zero-length element with Coulomb friction hysteresis was added in parallel at the beam-column connection to simulate friction (neoprene-concrete coefficient of friction, Magliulo et al. 2011, equal to 0.13 and elastic stiffness equal to 9.0 kN/mm). The friction connection between the roof elements and the supporting beams was similarly modelled (neoprene-concrete coefficient of friction equal to 0.11 and elastic stiffness equal to 2.3 kN/mm).

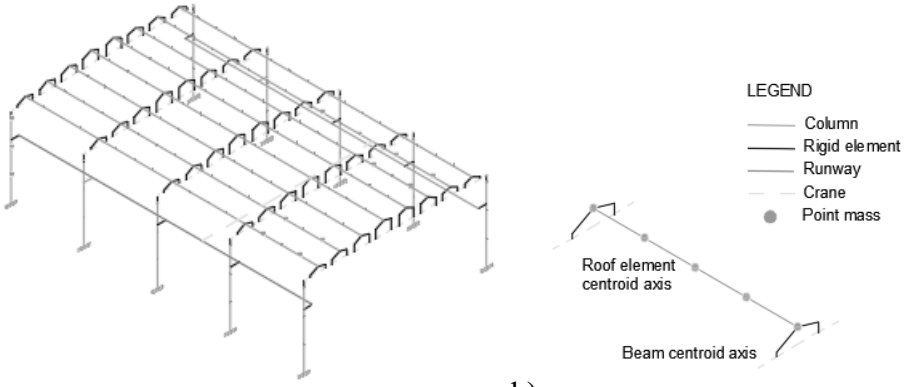

a) b)

Figure 4 – a) scheme of the 3D finite element model and b) detail of the roof elements.

Table 1 – Considered plastic hinge parameters according to the modified Ibarra-Medina-Krawinkler deterioration model [McKenna and Fenves 2013].

Column plastic hinge					
M_y	K_1	M_{max}	θ_y	K_2	M_u
458 kNm	22200 kNm/rad	614 kNm	0.026 rad	5994 kNm/rad	91.66 kNm
Beam-column connection					
F_y	K_1	F_{max}	Δ_y	K_2	F_u
54 kN	59600 kN/m	54 kN	0.14 mm	0 kN/m	0 kN

It is worth noting that the cladding panels were not directly modelled; only their masses were added on the supporting structural elements. The columns and the beams were subdivided in order to have nodes in correspondence to the cladding panel position. Cladding-beam connections are typically designed to allow sliding, however during a seismic event the locking of such connections might change the structural performance, attracting higher loads in the cladding connections with their possible failure. This effect is not considered in the paper. The column corbel was modelled as a rigid element simply-supporting the runway beams of the overhead cranes. The latter was modelled as a pinned element connecting the middle of the runway beams (**Figure 4a**), the payload was included

with the payload mass connected to the overhead crane trough horizontal springs and dampers in accordance with Belleri et al. (2017b): the elastic spring stiffness and the coefficient of damping were set equal to 80 kN/m and 0.001 Ns/m, respectively. Regarding the roof elements, since the depth of the beam changes along the beam height, a set of rigid elements (**Figure 4b**) was introduced in the model to simulate the position of the four supports of each roof element and to reach the beam centroid. The mass of each element was equally subdivided into the element nodes with the exception of the vertical cladding where only 1/3 of the mass was positioned at the beam nodes.

4. Loss estimation for existing buildings

The main vulnerabilities associated with seismic damage to both structural and non-structural elements were identified as a function of the pertaining EDPs. Various damage states (DS) were selected and the required repair actions and repair costs defined (**Table 2**). In particular, the considered vulnerabilities regard: the development of a plastic hinge at the column base as a function of the base rotation; the damage in the beam-column connection as a function of their horizontal relative displacements and the possible loss of support; the relative sliding between the roof elements and the supporting beams and their possible loss of support; the damage in the cladding panel connections as a function of the relative displacement of the cladding system with respect to the supporting elements. The dispersion (β) of the fragility curves was assumed 0.40 [FEMA P-58, 2012]. It should be noted that all the repair actions in **Table 2** are determined to restore the as-is situation before the seismic event, without any improvement with the exception of DS3 of the beam-column connection where a new connection is foreseen, since the replacement of the failed dowel is unfeasible. The repair costs in **Table 2** consider the costs associated with the raw materials, the equipment rental, the labour and the disposal according to the regional price lists for the public works in the Lombardia region and they should be considered as a lower bound estimate. The reported prices refer to the cost of the single elements; indeed, in the case of collapse of one of the lower elements in the collapse hierarchy, the collapse of all the supported elements is expected. In such conditions the cost associated with the collapse of all the supported elements will be automatically included in the loss evaluation procedure (Section 2).

Once all the parameters required for the application of the damage assessment procedure were defined, the DBLA procedure was applied to a simplified model (i.e. single column model) considering the new proposed collapse hierarchy. The procedure was validated by means of incremental dynamic analyses (IDA) [Vamvatsikos et al. 2006] carried out on both the simplified and the complete 3D model. Considering the simplified model, a single central column was selected (**Figure 5a**). The mass of the horizontal cladding was placed directly on the column at the cladding

connection position. Analogously, the mass of the runway beams and half of the mass of the overhead crane were placed on the corbel. The beam was modelled by means of a vertical stiff element (with height equal to the beam average height) on which half of the mass of the beam was applied. The top of the beam element was connected to a node resembling the mass of the roof tributary portion. The column plastic hinge, the beam-column connection, and the roof element connection were modelled as previously described.

Table 2 – Damage states and repair actions for the considered vulnerabilities for single elements.
* Derived from Hunt and Stojadinovic (2010)

DS	Damage description	EDP	Repair action	Cost (€)
Column plastic hinge				
1	Cracking	0.0377 rad	Epoxy resin injection	110
2	Concrete spalling	0.0290 rad	Replacement of concrete cover	120
3	Column failure	0.0350 rad	Column replacement	3190
Beam-column connection				
1	Column tip and beam end cracking	9.1 mm	Epoxy resin injection	160
2	Column and beam concrete spalling	11.1 mm	Replacement of concrete cover	170
3	Connection failure	28 mm	New connection	450
4	Beam loss of support	200 mm	Beam replacement	4170
Roof element				
1	Small relative displacement	30 mm	Replacement of 25% of the waterproofing system	40
2	Medium relative displacement	45 mm	Replacement of 50% of the waterproofing system	120
3	Loss of support	60 mm	Roof element replacement	920
Vertical cladding				
1	Yielding of the connection	35 mm	Connection replacement	210
2	Connection failure, panel overturning	55 mm	Panel replacement	1130
Horizontal cladding				
1	Yielding of the connection	10 mm	Connection replacement	210
2	Connection failure, panel overturning	45 mm	Panel replacement	1190
Cladding caulking (EDP relative displacement) *				
1	Damage of joint sealant	30 mm	Retrofit 50% of the joint sealant	95

A pushover analysis was conducted on the simplified model with a lateral force distribution according to the first mode. The pushover curve is represented in **Figure 5b**. The circles represent the relevant points of the DBLA procedure and they are associated with the operational limit state, the serviceability limit state, the activation of the roof element sliding and its loss of support. The results show that the roof elements start sliding at a displacement equal to 54mm until the loss of support (at 114 mm); therefore, in this displacement range there is no increase of the base shear. The elastic stiffness of the system (k=1130 kN/m) is directly obtained from the first branch of the pushover curve. This allows to derive the fundamental period of the system:

$$T_1 = 2\pi \cdot \sqrt{\frac{m}{k}} \quad (5)$$

where the equivalent mass (m) was taken equal to the total mass of the roof plus 1/3 of the mass acting on the columns (m = 29600 kg), similarly to what done for the vertical cladding panels. The effective period (T_{eff}) associated with the points selected on the pushover curve (**Figure 5b**) is obtained from applying the same equation.

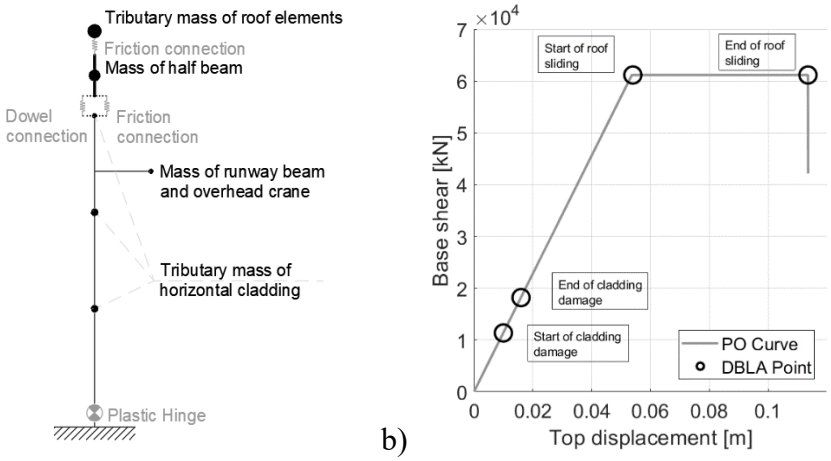

Figure 5 – (a) simplified model and (b) corresponding pushover curve

For each point, it is possible to evaluate the displacement ductility (μ_Δ), the effective damping (ξ_{eff}) and the spectral reduction factor (η) according to Priestley et al. (2007):

$$\mu_\Delta = \frac{\left(\frac{T_{eff}}{T_1}\right)^2 (1-r)}{\left(1-r\left(\frac{T_{eff}}{T_1}\right)\right)}, \quad \xi_{eff} = 0.05 + C \cdot \left(\frac{\mu_\Delta - 1}{\mu_\Delta \cdot \pi}\right), \quad \eta = \sqrt{\frac{0.1}{0.05 + \xi_{eff}}} \quad (6, 7, 8)$$

where r is the slope of the second branch of the pushover curve set equal to 0.0001 and C is a dimensionless coefficient accounting for the type of hysteresis considered, herein taken equal to 0.565 [Priestley et al. 2007]. **Table 3** shows the parameters associated with the selected points and the results of the DBLA procedure. The loss value is expressed as a fraction of the construction cost, herein taken as 108'000€.

Table 3 – Parameters of the DBLA procedure.
Note: MAFE is the mean annual frequency of exceedance. The results consider the collapse hierarchy.

I.D. Point	D (m)	K_{eff} (kN/m)	μ_Δ	ξ_{eff}	η	MAFE	Loss [%]
1	0.010	1130	1.00	0.050	1.00	0.03333	1.20
2	0.016	1130	1.00	0.050	1.00	0.02000	1.74
3	0.054	1130	1.00	0.050	1.00	0.00217	23.54
4	0.114	540	2.11	0.145	0.72	0.00039	34.91

From the loss and mean annual frequency of exceedance (MAFE) values of **Table 3,** it is possible to construct the loss curve obtained from the DBLA procedure and compare it with the IDA loss curve. As shown in **Figure 6**, the curve obtained from the DBLA procedure underestimates the expected losses for the analysed building. The EAL values obtained from the integral of the DBLA and IDA curves are 0.30% and 0.35% respectively, i.e. as a percentage of the building construction cost. It should be noted that by applying the DBLA procedure to the simplified column model, the behaviour of only one element for each typology is considered and the dispersion of the results due to the spatial variation of the output is not captured. Therefore, to account for this issue, the dispersion coefficient used in defining the damage state fragilities was increased from $\beta = 0.4$ to $\beta = 0.45$ similarly to what suggested in FEMA P-58-1 (2012). This produces a horizontal translation of the DBLA points. If the uncertainties associated with the variability of the seismic input are also accounted for, a vertical translation of the DBLA points is observed. The result obtained from considering such uncertainties is represented in **Figure 6** (DBLA uncert.) and the associated EAL is 0.52%. This overestimation of the results is due to the lack of intermediate points between the 2nd and 3rd points of the DBLA curve. To further improve the DBLA results, an intermediate limit state was considered with MAFE equal to 0.00714 (loss equal to 20%). The resulting curve is shown in **Figure 6** (DBLA refined) and the corresponding EAL is 0.357%, which matches well with the IDA value (0.356%). It is worth observing that the obtained value of EAL is 3 times greater than the value assumed by Babic and Dolsek (2019) for code conforming structures.

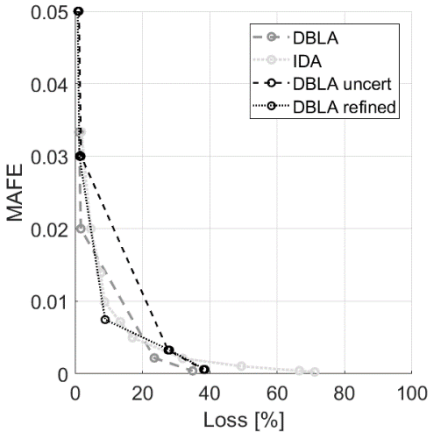

Figure 6 – Loss curves obtained from the DBLA and IDA procedures.

Figure 7a shows the mean damage factor (MDF) as a function of the seismic intensity expressed as the ratio of the spectral value at the period T_1, $S_a(T_1)$, and the corresponding value for the life safety limit state, $S_a(T_1)_{LS}$. It is interesting to note that the DBLA results (obtained from considering 9 limit states) reach at most the 60% of the damage estimated from the IDA curve. This is related to the activation of sliding of the roof elements and to the aforementioned uncertainties considerations. It is also worth observing that, if 40% is considered as the maximum damage factor before reconstruction

(FEMA P-58-1, 2012), the MDF is approximately linear up to this point. This aspect allows a simple closed form solution for the EAL estimation, similarly to what reported in Sullivan (2016). Finally, looking in detail at the damaged elements (**Figure 7b**), it is observed that the cladding panels are responsible for the loss values at the lower intensity measures; while the total collapse of the roof elements and of the vertical cladding panels and the partial collapse of the horizontal cladding system are responsible for the loss values at higher intensity levels. The beam-column connection, the column plastic hinge and the beam experience limited damage (less than 10%) due to the limited load increase following the activation of sliding of the roof elements.

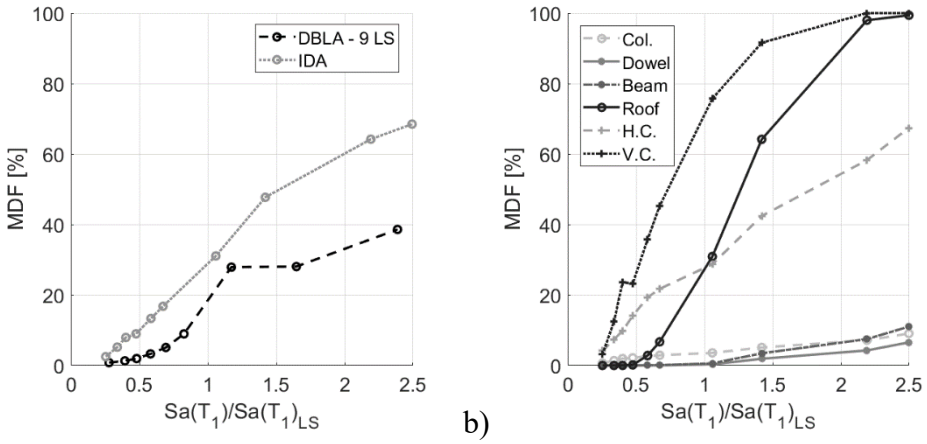

a) b)

Figure 7 – Mean Damage Factor (MDF) as a function of the seismic intensity.
Note: $S_a(T_1)$ is the spectral value at the period T1; $S_a(T_1)_{LS}$ is the spectral value for the Life Safety limit state; H.C. and V.C. are horizontal and vertical cladding respectively.

5. Retrofitting schemes and cost-benefit analyses

From the results presented in the previous section, it is observed that most of the economic losses are related to the collapse of the cladding panels. However, it is important to consider the collapse of the roof elements in respect to the life safety and to the possible damage to the building content such as industrial equipment and machinery, which could also affect indirect losses.

Given these considerations, the first considered retrofit strategy is the provision of a mechanical device (i.e. a steel bracket with 10mm diameter bolts) connecting each roof element to the supporting beam. The results of the application of the refined DBLA procedure described in the previous section are reported in **Table 4** and represented in **Figure 8**, showing a good correspondence with the IDA results: EAL equal to 0.41% compared to 0.42%.

Table 4 – Parameters of the DBLA procedure after retrofit of the roof elements.

I.D. Point	D (m)	K_{eff} (kN/m)	μ_Δ	ξ_{eff}	η	MAFE	Loss [%]
1	0.011	1134557	1.00	0.050	1.00	0.03333	0.85
2	0.016	1134557	1.00	0.050	1.00	0.02000	1.30
3	0.030	1134557	1.00	0.050	1.00	0.00714	8.82
4	0.055	1134557	1.00	0.050	1.00	0.00211	29.63
5	0.071	1017188	1.12	0.070	0.91	0.00103	49.02

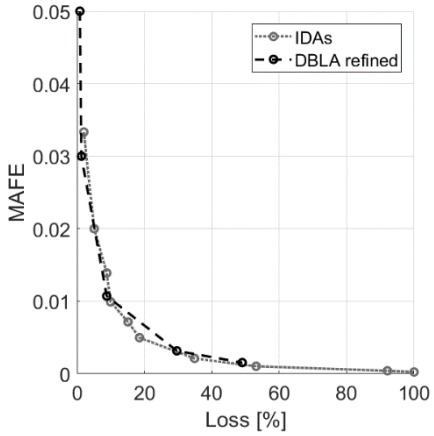

Figure 8 – Loss curve after the retrofit of the roof elements.

Very similar results are obtained from additionally improving the performance of the beam-column connection. It is particularly interesting to observe how, despite the improvements made to the structure, the EAL does not decrease. However, it is worth remembering how the evaluated losses do not include the building content which could be significantly damaged by the loss of support and subsequent falling of the roof elements. In such conditions the EAL of the non-retrofitted building would be much higher. At this regard, **Figure 9** shows the collapse probability, considering the collapse hierarchy, of the roof elements before and after retrofit of the roof elements, after the additional retrofit of the beam-column connection and after the additional retrofit of the column base. It is observed how the collapse probability is reduced after the roof elements retrofit (i.e. by placing a mechanical device to avoid sliding); the additional retrofit of the beam-column connection does not produce benefits. The collapse probability is significantly reduced only after increasing the column rotational capacity. It is worth noting that applying the DBLA procedure without accounting for the collapse hierarchy leads to an underestimation of the collapse probability of about 50%.

Figure 10 shows the MDF as a function of the seismic intensity after the roof elements retrofit (**Figure 10a**). After the additional retrofit of the beam-column connection the curves are practically the same as in **Figure 10a.** A significant decrease of MDF is observed after the retrofit of the cladding system and of the column rotational capacity (**Figure 10b**). It is interesting to observe that the increase of the seismic load transferred by the roof leads to an increase of damage in the supporting elements.

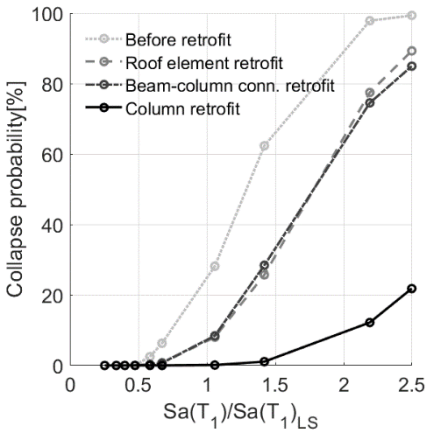

Figure 9 – Collapse probability of the roof elements before and after retrofit.

To obtain a reduction of EAL, it is necessary to define retrofit interventions to reduce losses for lower intensity levels: retrofitting the cladding system by providing additional steel brackets with slotted holes to allow the relative sliding between the panel and the supporting structure. The results are shown in **Figure 11**. The EAL after the additional retrofit of the cladding system becomes 0.12%. It is worth observing that, after the retrofit of the connection between the cladding and the supporting elements, the MDF as a function of the seismic intensity (**Figure 11b**) is approximately constant up to an intensity level of about 70% of the life safety limit state and then linear until full collapse. In the case of column retrofit with steel brackets to increase the ultimate rotation capacity (0.065rad), the value of EAL is equal to 0.054%. The probability of collapse is less than 1% at the life safety limit state and increases to 20% for a return period of 4175 years.

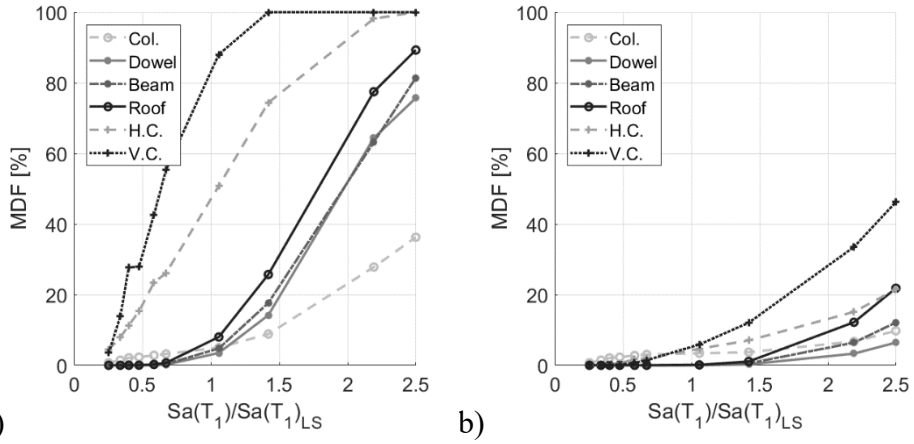

Figure 10 - Mean Damage Factor (MDF) as a function of the seismic intensity for the retrofit of the roof elements (a) and of the additional retrofit of the beam-column connection, cladding system, and column base (b).

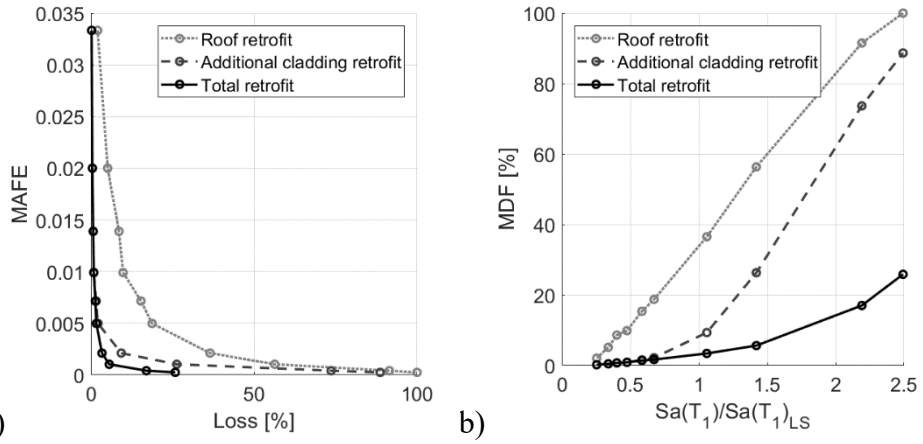

Figure 11 – Loss curve (a) and Mean Damage Factor (b) after retrofit of the roof elements and beam connections and after the additional retrofit of the cladding system.

Figure 12 shows a scheme of the considered retrofit interventions. The whole cost associated with each intervention is equal to 1800€, 3600€, 2000€, and 3000 € for the roof elements, beam-column connections, connection of the cladding system to the supporting element, and columns, respectively (adapted from Fianchisti 2012).

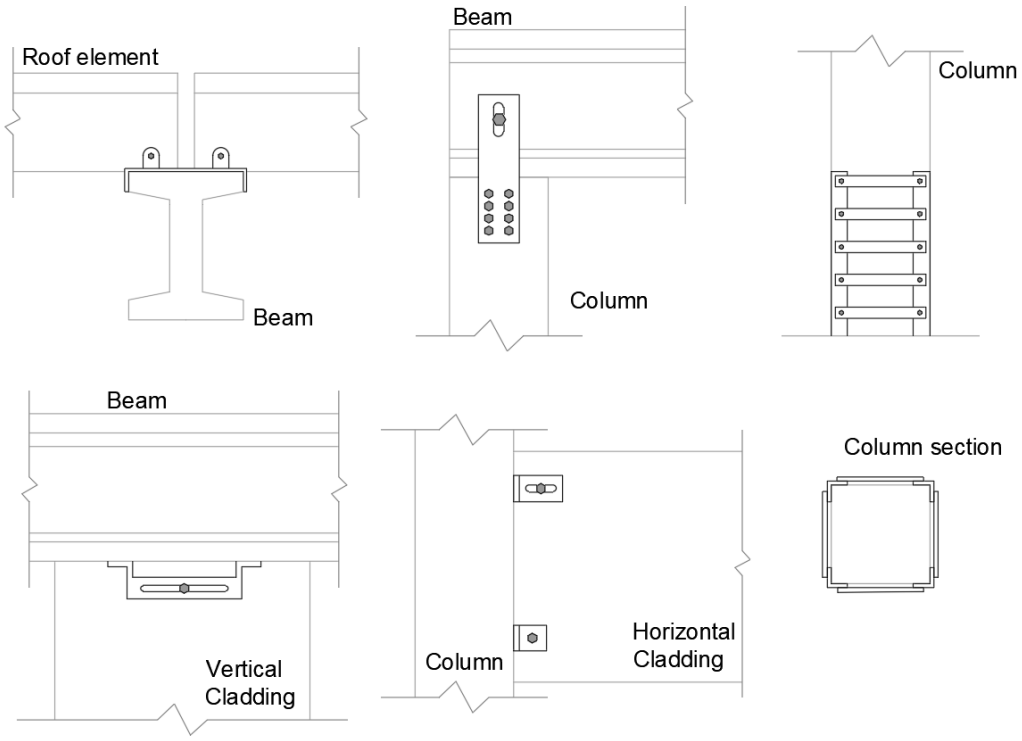

Figure 12 – Retrofit interventions.

A breakeven analysis has been conducted to evaluate the effectiveness of the retrofit intervention. Expected benefits have been discounted over the building life span (assumed 50 years) to obtain the net present value (NPV) of the investment:

$$NPV = \sum_{t=1}^{Tb} \frac{\Delta_{EAL}}{(1+r)^t} - C_{ret} \qquad (9)$$

where r is the rate of return, equal to 0.01 [Cardone et al. 2019], T_b is the building life span, C_{rIet} is the total retrofit cost and Δ_{EAL} is the EAL variation before and after retrofit. By placing NPV equal to zero, it is possible to obtain the return period of the investment (i.e. the breakeven time), herein equal to 27 years. It is worth noting that this value does not include the savings obtained from avoided damage to the equipment and machinery. If we consider a machinery cost of 250'000€ located under the central bay, and therefore damaged in the case of collapse of the roof elements, assessed as the mean probability of collapse of the roof elements considering the collapse hierarchy, it is observed that the savings derived from the whole retrofit produce a breakeven time of 12 years.

6. Conclusions

This paper shows the results obtained from the application of the displacement-based loss assessment (DBLA) procedure to typical precast industrial and commercial buildings in the Italian territory. In particular, a collapse hierarchy is introduced to capture the partial collapses typical of the considered structural typology. The damage assessed herein is the direct loss of the structural and non-structural elements (i.e. external cladding system). However, it should be noted that the damage to the building content (e.g. equipment and machinery) and the indirect losses related to the building inactivity may exceed the value of the direct losses.

The considered buildings typology, built before the enforcement of modern building codes without accounting for any seismic provision or relying on non-updated seismic zonation, experiences substantial damage in case of earthquakes due to the onset and effects of local collapse mechanisms, such as the loss of support of the beams and of the roof elements. It has been observed that the traditional DBLA method enables a good estimate of the damage as long as the local mechanisms, such as friction between elements, have not been activated. The DBLA procedure has been applied to a simplified model considering an inner column and a schematic representation of the supported elements, by lumping all the inelasticity at a single connection for each element typology and by considering the appropriate tributary mass.

Comparing the DBLA results with the results obtained from an incremental dynamic analysis (IDA), it is observed that the two curves present a similar linear trend until the onset of the local collapse mechanism (i.e. friction between the roof elements and the supporting beam), although there is a significant underestimation of the expected loss in case of the DBLA procedure. This is due to the uncertainties related to the seismic input and to the variation of the seismic output in the structural elements, not available in the simplified model. To account for such aspects, the dispersion of the damage fragility was increased (from 0.4 to 0.45) and the variability of the seismic input was included by means of the SAC/FEMA procedure as modified by Fajfar and Dolsek (2010). The inclusion of

uncertainties in the DBLA procedure and the introduction of an intermediate limit state (between the serviceability and the life safety limit states) for the loss evaluation lead to DBLA results matching quite well with the IDA values.

It is worth noting that as long as the local collapse of the elements is triggered at a damage level exceeding 40% of the construction costs, the expected annual loss (EAL) can be evaluated in a closed form [Welch et al. 2014] due to the linear variation of the loss values with respect to the seismic intensity. Indeed, for damage level greater than 40% there is no economic advantage in repairing the building compared to reconstruction. This aspect can be included in the simplified evaluation of EAL.

Regarding the seismic retrofit of the considered building typology, it is observed that both economic losses reduction and life safety need to be pursued. In particular, when the retrofit of the local mechanisms of the roofing system is carried out, the collapse probability of the roof elements at the life safety limit state drops form 27% before retrofit to 7% after the retrofit, while the EAL remains approximately constant, being governed by the damage of the cladding systems for low intensity earthquakes. The additional retrofit of the column base, by increasing its rotation capacity, reduces the collapse probability to values less than 1%. On the other end, to effectively reduce the EAL it is necessary to retrofit those elements that mostly affect the economic loss for low seismic intensity values, such as the cladding system. After the whole retrofit process, the EAL for the selected case study drops from 0.36% to 0.05% of the construction cost.

Acknowledgements

The contribution of Eng. M. Bassetti and Eng. M.E. Bressanelli in setting up the OpenSees and Matlab model is gratefully acknowledged. The study presented in this article was developed within the activities of the ReLUIS-DPC 2014-2018 research program. Opinions and conclusions do not necessarily reflect those of the funding entity and of the people acknowledged.

Appendix

Figure 13 shows the response spectrum of the accelerograms used in the non-linear time history analyses: the continuous grey line represents the response spectrum for each earthquake, the continuous black line the average spectrum and the dotted black line the building code elastic response spectrum [D.M. 14/01/2008].

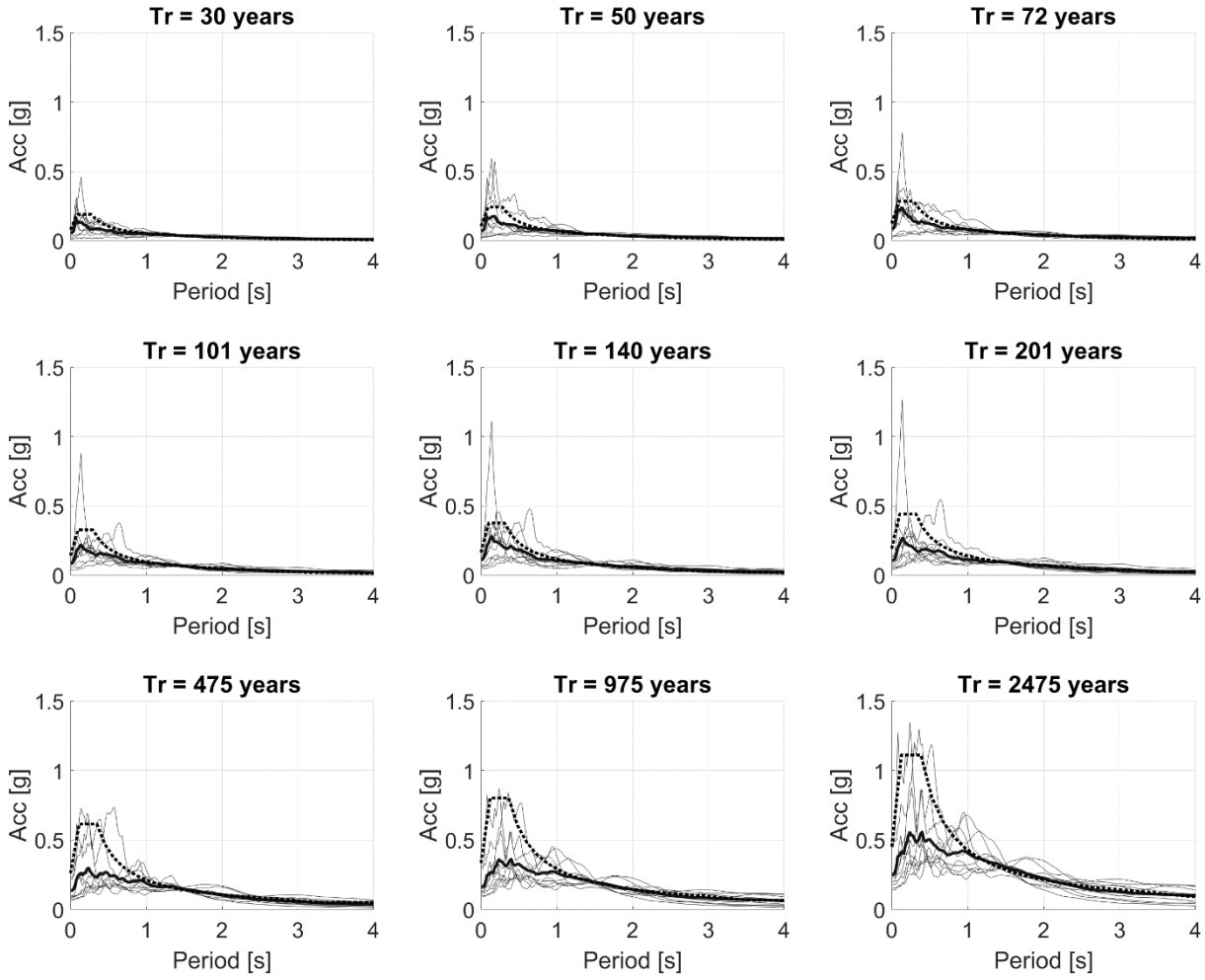

Figure 13 – Response spectra for each considered return period.

References

Babič A., Dolšek M. [2019]. "*A five-grade grading system for the evaluation and communication of short-term and long-term risk posed by natural hazards". Structural safety*, 78:48-69

Georios Baltzopoulos G., Baraschino R., Iervolino I., Vamvatsikos D. [2017]. "*SPO2FRAG: software for seismic fragility assessment based on static pushover." Bulletin of Earthquake Engineering,* 15:4399-4425

Baker J.W. [2011]. *"Conditional Mean Spectrum: Tool for Ground-Motion Selection." Journal of Structural Engineering,* 137(3):322-331.

Belleri A., Riva P. [2012]. *"Seismic Performance and Retrofit of Precast Concrete Grouted Sleeve Connections", PCI Journal,* 57(1):97-109

Belleri A., Brunesi E., Nascimbene R., Pagani M., Riva P. [2014]. *"Seismic Performance of Precast Industrial Facilities Following Major Earthquakes in the Italian Territory." J. Perform. Constr. Facil.,* doi:10.1061/(ASCE)CF.1943-5509.0000617

Belleri A., Torquati M., Riva P., Nascimbene R. [2015]. *"Vulnerability assessment and retrofit solutions of precast industrial structures." Earthquake and Structures,* 8(3):801-820

517 Belleri A., Torquati M., Marini A., Riva P. [2016]. "*Horizontal cladding panels: in-plane seismic*
518 *performance in precast concrete buildings." Bulletin of Earthquake Engineering*, 14: 1103-1129

519 Belleri A., Cornali F., Passoni C., Marini A., Riva P. [2017b]. *"Evaluation of out-of-plane seismic*
520 *performance of column-to-column precast concrete cladding panels in one-storey industrial*
521 *buildings." Journal of Earthquake Engineering and Structural Dynamics*, 47:397-417

522 Belleri A., Labò S., Marini A., Riva P. [2017b]. *"The influence of overhead cranes in the seismic*
523 *performance of industrial buildings". Frontiers in Built Environment, section Earthquake*
524 *Engineering*, 3(64).

525 Belleri A. [2017]. *"Displacement based design for precast concrete frames with not-emulative*
526 *connections." Engineering Structures*, 141:228-240

527 Bournas D.A., Negro P., Taucer F. [2014]. *"Performance of industrial buildings during the Emilia*
528 *earthquakes in Northern Italy and recommendations for their strengthening." Bulletin of Earthquake*
529 *Engineering*, 12(5):2383-2404

530 Brunesi E., Nascimbene R., Bolognini D., Bellotti D. [2015]. *"Experimental investigation of the*
531 *cyclic response of reinforced precast concrete framed structures." PCI Journal*, 15(2):57-79

532 Cardone D., Gesualdi G., Perrone G. [2019]. "*Cost-Benefit Analysis of Alternative Retrofit*
533 *Strategies for RC Frame Buildings." Journal of Earthquake Engineering*, 23(2):208-241

534 Casotto C., Silva V., Crowley H., Nascimbene R., Pinho R. [2015]. *"Seismic Fragility of Italian*
535 *RC Precast Industrial Structures." Engineering Structures,* 94:122-136

536 Colombo A., Negro P., Toniolo G., Lamperti M. [2016]. *"Design guidelines for precast structures*
537 *with cladding panels." JRC Technical report,* ISBN 978-92-79-58534-0

538 Clementi F., Scalbi A., Lenci S. [2016]. "*Seismic performance of precast reinforced concrete*
539 *buildings with dowel pin connections." Journal of Building Engineering,* 7: 224-238
540 DOI:10.1016/j.jobe.2016.06.013

541 Cornell C.A., Jalayer F., Hamburger R.O., Foutch D.A. [2002]. *"Probabilistic basis for 2000 SAC*
542 *Federal Emergency Management Agency, Steel Moment Frame Guidelines." Journal of Structural*
543 *Engineering,* 128(4):526-553

544 Cremen G., Baker J.W. [2019]. *"A Methodology for Evaluating Component-Level Loss*
545 *Predictions of the FEMA P-58 Seismic Performance Assessment Procedure." Earthquake Spectra*,
546 35(1):193-210

547 Dal Lago B., Toniolo G., Lamperti M. [2016]. *"Influence of different mechanical column-*
548 *foundation connection devices on the seismic behaviour of precast structures." Bull Earthq Eng.,*
549 14(12):3485-3508

550 Dal Lago B., Bianchi S., Biondini F. [2019]. *"Diaphragm effectiveness of precast concrete*
551 *structures with cladding panels under seismic action." Bulletin of Earthquake Engineering,*
552 17(1):473-495

553 Del Vecchio C., Di Ludovico M., Pampanin S., Prota A. [2018]. *"Repair Costs of Existing RC*
554 *Buildings Damaged by the L'Aquila Earthquake and Comparison with FEMA P-58 Predictions."*
555 *Earthquake Spectra*, 34(1):237-263

556 Demartino C., Vanzi I., Monti G., Sulpizio C. [2018]. *"Precast industrial buildings in Southern*
557 *Europe: loss of support at frictional beam-to-column connections under seismic actions." Bulletin of*
558 *Earthquake Engineering*, 16(1):259-294

559 D.M. 14/01/2008, *"Norme Tecniche per le Costruzioni." Gazzetta Ufficiale della Repubblica*
560 *Italiana,* 29, 2008.

561 Fajfar P., Dolsek M. [2010]. "*A Practice-Oriented Approach for Probabilistic Seismic Assessment.*
562 *Advances in Performance-Based Earthquake Engineering", Springer, Edited by M.N. Fardis,* 225-
563 233

564 FEMA P-58-1 [2012]. *Seismic Performance Assessment of Buildings, Volume 1 – Methodology,*
565 *Applied Technology Council*

566 FEMA P-58-3.1 [2016]. *Seismic Performance Assessment of Buildings Volume 3—Performance*
567 *Assessment Calculation Tool (PACT)* Version 2.9.65, APPLIED TECHNOLOGY COUNCIL

568 Fianchisti G. [2012]. "*Prezziario di riferimento per gli interventi locali e globali su edifici*
569 *industriali monopiano non progettati con criteri antisismici di cui alle linee di indirizzo del*
570 *19.06/2012, v. 1.0 Protezione Civile" – Reluis –* CNI – ASSOBETON

571 Hunt J.P., Stojadinovic B. [2010]. *"Seismic Performance Assessment and Probabilistic Repair*
572 *Cost Analysis of Precast Concrete Cladding Systems for Multistory Buildings." Pacific Earthquake*
573 *Engineering Research Center,* Report 2010/110

574 Günay M., Mosalam K. [2012]. *"PEER Performance Based Earthquake Engineering*
575 *Methodology" Revisited, J. Earthq. Eng.*, 17(6):829–858

576 Krawinkler H., Miranda E. [2004]. *Performance-Based Earthquake Engineering, in Earthquake*
577 *Engineering, Edited by., no. Ch. 9, International Code Council (ICC), Ed. Boca Raton London New*
578 *York Washington, D.C.: CRC PRESS*, pp. 560–635

579 Kremmyda G.D., Fahjan Y.M., Tsoukantas S.G. [2014]. "Nonlinear FE analysis of precast RC
580 pinned beam-to-column connections under monotonic and cyclic shear loading." Bulletin of
581 Earthquake Engineering, 12: 1615-1638

582 Kremmyda G.D., Fahjan Y.M., Psycharis I.N., Tsoukantas S.G. [2017]. "*Numerical investigation*
583 *of the resistance of precast RC pinned beam-to-column connections under shear loading."*
584 *Earthquake Engng Struct. Dyn.*, doi: 10.1002/eqe.2868

585 Kunnath S.K., Larson L., Miranda E. [2006]. *"Modelling Considerations in Probabilistic*
586 *Performance-based Seismic Evaluation: Case study of the I-880 viaduct", Earthq. Eng. Struct. Dyn.,*
587 35(1):57–75.

588 Magliulo G., Bellotti D., Cimmino M., Nascimbene R. [2018]. "Modeling and Seismic Response
589 Analysis of RC Precast Italian Code-Conforming Buildings." Journal of Earthquake Engineering,
590 22(sup2):140-167

591 Magliulo G., Capozzi V., Fabbrocino G., Manfredi G. [2011]. *"Neoprene–concrete friction*
592 *relationships for seismic assessment of existing precast buildings." Engineering Structures,* 33:532–
593 538

Magliulo G., Ercolino M., Petrone C., Coppola O., Manfredi G. [2014a]. *"The Emilia Earthquake: Seismic Performance of Precast Reinforced Concrete Buildings." Earthquake Spectra,* 30(2):891-912

Magliulo G., Ercolino M., Cimmino M., Capozzi V., Manfredi G. [2014b]. *"FEM analysis of the strength of RC beam-to-column dowel connections under monotonic actions." Construction and Building Materials,* 69:271–284

McKenna F., Fenves G.L., *"OpenSees Manual. Pacific Earthquake Engineering Research center."* 2013.

Minghini F., Ongaretto E., Ligabue V., Savoia M., Tullini N. [2016]. *"Observational failure analysis of precast buildings after the 2012 Emilia earthquakes." Earthquake and Structures,* 11(2):327-346

Nastri E., Vergato M., Latour M. [2017]. "*Performance evaluation of a seismic retrofitted R.C. precast industrial building." Earthquakes and Structures*, 12(1):13-21

Palanci M., Senel S.M., Kalkan A. [2017]. "*Assessment of one story existing precast industrial buildings in Turkey based on fragility curves." Bulletin of Earthquake Engineering,* 15(1):271-289

Papadopoulos A.N., Vamvatsikos D., Kazantzi A.K. [2019]. "*Development and Application of FEMA P-58 Compatible Story Loss Functions. Earthquake Spectra",* 35(1):95-112

Priestley M.J.N., Calvi G.M., Kowalsky M.J. [2007]. "*Displacement-Based Seismic Design of Structures." IUSS Press, Pavia, Italy*

Savoia M., Mazzotti C., Buratti N., Ferracuti B., Bovo M., Ligabue V., Vincenzi L. [2012]. "*Damages and collapses in industrial precast buildings after the Emilia earthquake." Ingegneria Sismica*, 29(2-3):120-131

Scotta R., De Stefani L., Vitaliani R. [2015]. *"Passive control of precast building response using cladding panels as dissipative shear walls." Bulletin of Earthquake Engineering*, 13(11):3527-3552

Sullivan T.J. [2016]. *"Use of Limit State Loss versus Intensity Models for Simplified Estimation of Expected Annual Loss." Journal of Earthquake Engineering*, 20(6): 954-974

Toniolo G., Colombo A. [2012] *"Precast concrete structures: the lessons learned from the L'Aquila earthquake." Structural Concrete,* 13(2):73-83

Torquati M., Belleri A., Riva P. [2018]. *"Displacement-Based Seismic Assessment for Precast Concrete Frames with Non-Emulative Connections." Journal of Earthquake Engineering*, doi:10.1080/13632469.2018.1475311

Vamvatsikos D., Cornell A.C. [2006]. *"Direct estimation of the seismic demand and capacity of oscillators with multi-linear static pushovers through IDA." Earthq. Eng. Struct. Dyn.,* 35:1097–1117

Welch D.P., Sullivan T.J., Calvi G.M. [2014]. *"Developing Direct Displacement- Based Procedures for Simplified Loss Assessment in Performance-Based Earthquake Engineering." Journal of Earthquake Engineering*, 18: 290–322

Xu Z., Zhang H., Lu X., Xu Y., Zhang Z., Li Y. [2019]. *"A prediction method of building seismic loss based on BIM and FEMA P-58." Automation in Construction*, 102:245-257

632 Zoubek B., Fischinger M., Isakovic T. [2015]. *"Estimation of the cyclic capacity of beam-to-*
633 *column dowel connections in precast industrial buildings." Bulleting of Earthquake Engineering*,
634 13:2145–2168

635 Zoubek B., Fischinger M., Isaković T. [2016]. *"Cyclic response of hammer-head strap cladding-*
636 *to-structure connections used in RC precast building." Engineering Structures*, 119:135-148